

Lithium Diisopropylamide-Mediated Lithiations of Imines: Insights into Highly Structure-Dependent Rates and Selectivities

Songping Liao and David B. Collum*

Contribution from the Department of Chemistry and Chemical Biology, Baker Laboratory, Cornell University, Ithaca, New York 14853-1301

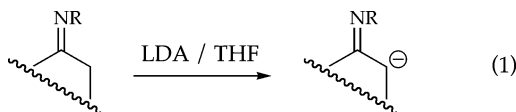
Received July 8, 2003; E-mail: dbc6@cornell.edu

Abstract: Lithium diisopropylamide-mediated lithiations of *N*-alkyl ketimines derived from cyclohexanones reveal that simple substitutions on the *N*-alkyl side chain and the 2-position of the cyclohexyl moiety afford a 60,000-fold range of rates. Detailed rate studies implicate monosolvated monomers at the rate-limiting transition structures in all instances. Comparisons of experimentally derived regioselectivities and rates, taken in conjunction with density functional theory computational studies, reveal a number of factors that influence reactivities including: (a) axial versus equatorial disposition of the proton on the cyclohexane ring, (b) syn versus anti orientation of the lithiation relative to the *N*-alkyl group, (c) the presence or absence of a potentially chelating methoxy moiety on the *N*-alkyl group, (d) the presence of a 2-methyl substituent at the geminal or distal α -carbon, and (e) branching in the *N*-alkyl group. The isolated contributions are not large, yet they display a strong and predictable additivity leading to a kinetic resolution of imines derived from racemic 2-methylcyclohexanone.

Introduction

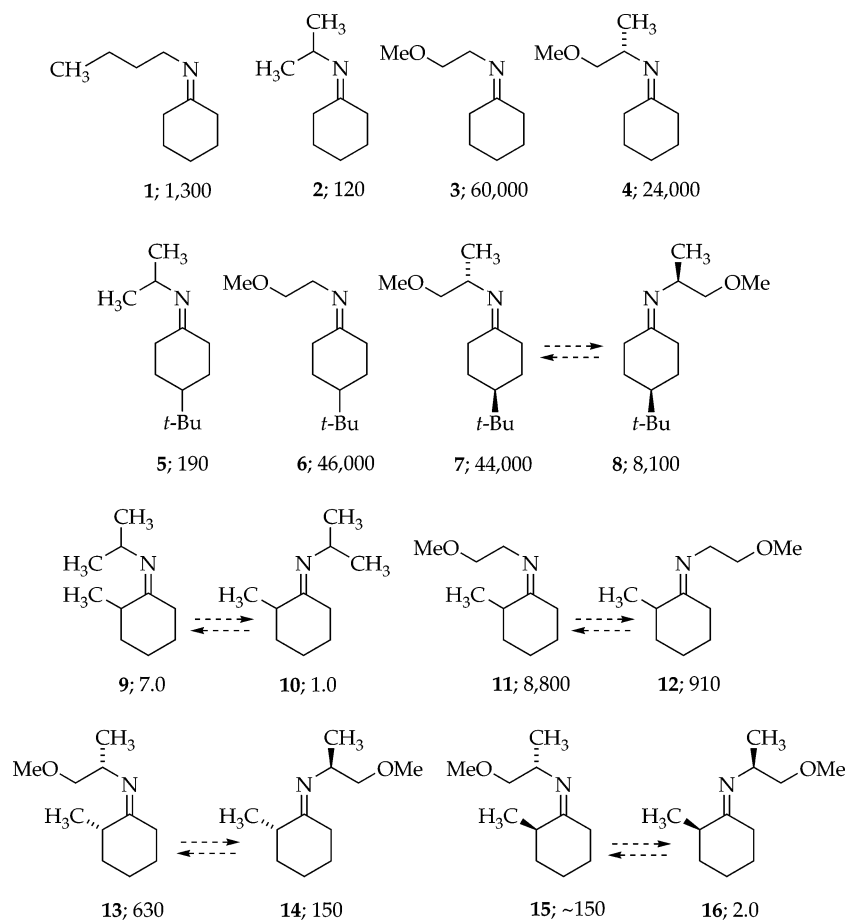
The organolithium chemistry of imines has played a central role in synthetic organic chemistry.^{1–3} Although imines and lithioimines appear to be functionally equivalent to ketones and ketone enolates, their reactivities are quite different. Imine lithiations are orders of magnitude slower than the analogous ketone enolizations,⁴ and the resulting lithioimines are substantially more reactive toward electrophiles than are their enolate counterparts.^{2,3} Self-condensations during the lithiations of imines are almost nonexistent due to the markedly lower electrophilicity of the imine C=N moiety as compared to the ketone C=O moiety.⁵ Of particular importance, the *N*-alkyl substituents on imines and lithioimines markedly influence their

reactivity and offer a vehicle to control reactivity and selectivity unavailable to ketones and ketone enolates.^{1,2} The favorable properties of imines and lithioimines that have captured the imagination of synthetic chemists also make them excellent templates for mechanistic studies.⁶ We illustrate this point by foreshadowing results summarized in Chart 1 and Scheme 1. Chart 1 contains structurally related imines along with relative rate constants (k_{rel} ; in parentheses) for the lithium diisopropylamide (LDA)-mediated lithiations (eq 1). Seemingly minor structural variations afford a striking 60 000-fold range of relative reactivities. In addition, results emerged that were not predicted based on previous studies:⁶ (1) LDA/THF-mediated lithiation of a 1:1 mixture of diastereomeric imines shown in Scheme 1 proceeds with a 75:1 preference for the lithiation of one diastereomer, and (2) lithiation occurs predominantly at the more substituted α -carbon. Further investigation of LDA-mediated lithiations of the imines in Chart 1 reveals structure–reactivity relationships that display surprising additivity.



- (1) Recent reviews describing some organolithium chemistry of imines: Denmark, S. E.; Nicaise, O. J.-C. In *Comprehensive Asymmetric Catalysis*; Jacobsen, E. N., Pfaltz, A., Yamamoto, Y., Eds; Springer-Verlag: Heidelberg, 1999; Chapter 26.2. Kobayashi, S.; Ishitani, H. *Chem. Rev.* **1999**, *99*, 1069. Enders, D.; Reinhold, U. *Tetrahedron: Asymmetry* **1997**, *8*, 1895. Volkmann, R. A. In *Comprehensive Organic Synthesis*; Trost, B. M., Fleming, I., Eds; Pergamon: Oxford, 1991; Chapter 1.12. Bloch, R. *Chem. Rev.* **1998**, *98*, 1407.
- (2) For general reviews on the chemistry of lithiated imines, see: Bergbreiter, D. E.; Momongan, M. In *Comprehensive Organic Synthesis*; Trost, B. M., Fleming, I., Eds; Pergamon: New York, 1989; Vol. 2, p 503. Martin, S. F. In *Comprehensive Organic Synthesis*; Trost, B. M., Fleming, I., Eds.; Pergamon: New York, 1989; Vol. 1, p 475. Hickmott, P. W. *Tetrahedron* **1982**, *38*, 1975. Enders, D. In *Current Trends in Organic Synthesis*; Nozaki, H., Ed.; Pergamon: New York, 1983. Whitesell, J. K.; Whitesell, M. A. *Synthesis* **1983**, 517. Also, see ref 3.
- (3) Fraser, R. R. In *Comprehensive Carbanion Chemistry*; Buncl, E., Durst, T., Eds.; Elsevier: New York, 1980.
- (4) By comparison, whereas LDA/THF lithiates simple imines of cyclohexanone slowly below 0 °C, enolizations of cyclohexanone are too fast to monitor at –78 °C.
- (5) Huryn, D. M. In *Comprehensive Organic Synthesis*; Trost, B. M., Fleming, I., Eds.; Pergamon: New York, 1991; Vol. 1, Chapter 1.2.

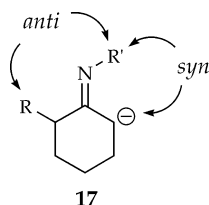
- (6) (a) Wanat, R. A.; Collum, D. B.; Van Duyne, G.; Clardy, J.; DePue, R. T. *J. Am. Chem. Soc.* **1986**, *108*, 3415. (b) Kallman, N.; Collum, D. B. *J. Am. Chem. Soc.* **1987**, *109*, 7466. (c) Bernstein, M. P.; Romesberg, F. E.; Fuller, D. J.; Harrison, A. T.; Williard, P. G.; Liu, Q. Y.; Collum, D. B. *J. Am. Chem. Soc.* **1992**, *114*, 5100. (d) Bernstein, M. P.; Collum, D. B. *J. Am. Chem. Soc.* **1993**, *115*, 789. (e) Bernstein, M. P.; Collum, D. B. *J. Am. Chem. Soc.* **1993**, *115*, 8008. (f) Romesberg, F. E.; Collum, D. B. *J. Am. Chem. Soc.* **1995**, *117*, 2166. (g) Ma, Y.; Collum, D. B., unpublished.

Chart 1. Relative Rate Constants for LDA/THF-Mediated Lithiations at $-40\text{ }^{\circ}\text{C}$ 

Literature Background

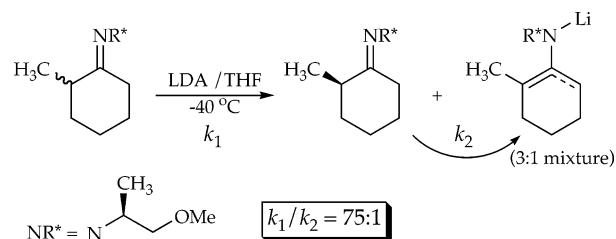
It is instructive to preface the results with a brief survey of the literature germane to understanding the mechanism of LDA-mediated imine lithiations. Because the chemistry of ketimines differs considerably from that of their aldimine, hydrazone, oxime, and oximino ether counterparts,^{2,3} we focus solely on the *N*-alkyl ketimines.

Syn–Anti Stereochemistry. The consequences of the stereochemistry about the C=N bond of imines and lithioimines reviewed by Fraser³ can be quite confusing due to a large number of related issues. In particular, syn and anti are used to refer to the stereochemical relationship of the *N*-alkyl moiety relative to (1) a substituent on an unsymmetrical substrate, (2) the site of deprotonation, (3) location of the substituent introduced through alkylation, and (4) placement of the carbanionic carbon of the resulting lithioimine. Past debates and lingering issues are summarized as follows.



(1) Previous workers investigated the relative preference for the syn versus anti orientation in unsymmetrical imines as well as the mechanism of the syn–anti isomerization.³ Because the

Scheme 1

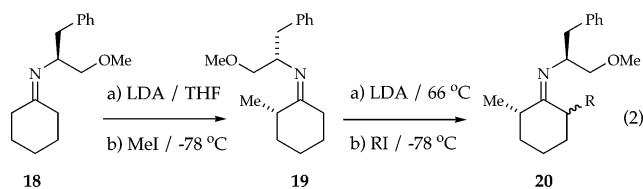


half-life for syn–anti isomerization is typically ≥ 0.5 h at $25\text{ }^{\circ}\text{C}$,^{3,7–9} the stereochemistry of the C=N bond can influence the reactions of imines.¹⁰

(2) After some early confusion about whether lithiations occur syn or anti to the *N*-alkyl moiety of imines and related Schiff's bases, the groups of Bergbreiter, Newcomb, and Meyers meticulously investigated lithiations of acyclic ketimines and found that the regiochemistry depended on a number of factors including the steric demands of the *N*-alkyl group as well as temperature.¹⁰ Subsequent semiempirical calculations revealed

- (7) Knorr, R.; Hintermeyer-Hilpert, M.; Böhrer, P. *Chem. Ber.* **1990**, *123*, 1137.
- (8) Fraser, R. R.; Banville, J.; Akiyama, F.; Chuaqui-Offermans, N. *Can. J. Chem.* **1981**, *59*, 705.
- (9) Leading references: Jennings, W. B.; Boyd, D. R. *J. Am. Chem. Soc.* **1972**, *94*, 7187. Boyd, D. R.; Jennings, W. B.; Waring, L. C. *J. Org. Chem.* **1986**, *51*, 992.
- (10) Steinig, A. G.; Spero, D. M. *Org. Prep. Proced. Int.* **2000**, *32*, 205.
- (11) Willoughby, C. A.; Buchwald, S. L. *J. Am. Chem. Soc.* **1994**, *116*, 11703.
- (12) (a) Smith, J. K.; Bergbreiter, D. E.; Newcomb, M. *J. Am. Chem. Soc.* **1983**, *105*, 4396. (b) Smith, J. K.; Newcomb, M.; Bergbreiter, D. E.; Williams, D. R.; Meyers, A. I. *Tetrahedron Lett.* **1983**, *24*, 3559. (c) Smith, J. K.; Bergbreiter, D. E.; Newcomb, M. *J. Org. Chem.* **1981**, *46*, 3158.

little inherent syn–anti preferences in the deprotonation,^{6f} yet they focused on the lithiations anti to the *N*-alkyl moiety. Lithiations of imines derived from unsymmetrically substituted ketones are complex due to the superposition of syn–anti preferences and steric effects. Lithiations often occur at the less substituted site^{10–12} as illustrated by the conversion of **19** to **20** (eq 2).¹³ The regioselectivity seems logical in light of highly regioselective LDA-mediated ketone enolizations.¹⁴ Nonetheless, lithiations at the more substituted positions of imines have been reported, the most compelling cases being those reported by Sakurai and co-workers.¹⁵ The asymmetric alkylations reported by Meyers and co-workers (eq 2) are especially pertinent.¹³ Although it was unclear to Meyers whether the isomerization of syn imine **19** to the anti isomer occurred before or after lithiation, the methyl moiety in **19** appeared to retard lithiation.

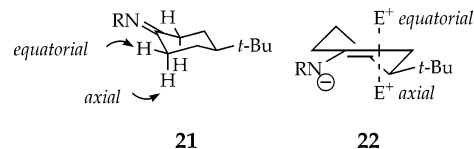


(3) There appears to be consensus that lithioimines alkylate syn to the *N*-alkyl moiety as illustrated in eq 2.^{3,10,16,17} Nonetheless, the origins of the effect have been a topic of considerable debate.

(4) The syn alkylations have been attributed to a high preference for the lithioimine to orient the *N*-alkyl moiety syn to the carbanion.^{3,17} Subsequent solid-state and solution-phase structural studies of an *N*-phenyl lithioimine confused the issue by showing that the *N*-phenyl moiety was neither syn nor anti to the carbanionic carbon but rather skewed out of the C=C–N plane in a dimeric structure.^{6a,b} Moreover, some concern arose that the dimers and monomers characterized by NMR spectroscopy^{6a,b} might have been misassigned as conformational isomers.¹⁸ We hasten to add, however, that the relationship of *N*-phenyl lithioimines to the *N*-alkyl lithioimines remains

unclear. Glazer and Streitwieser suggested that syn alkylations may derive from aggregation effects.¹⁶

Stereoelectronic Effects. The relative reactivities of axial and equatorial positions on cyclohexane ring systems—so-called stereoelectronic effects—have received considerable attention.^{3,19} Although we have not uncovered support in the literature for axially selective deprotonation of imines (**21**),²⁰ the resulting lithioimines display a high propensity to alkylate axially (**22**).^{3,21}



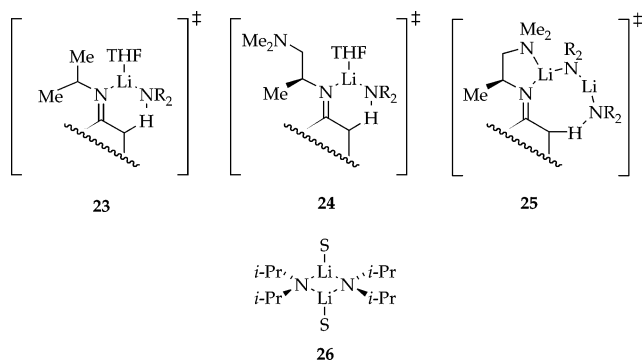
Mechanisms of Lithiation. Most studies of the lithiation and alkylation of imines offer no insight into the underlying organolithium chemistry. In contrast, we became interested in exploiting the imines as vehicles to investigate organolithium chemistry without becoming embroiled in debates about the syn effect and other substrate-centric issues. A series of rate studies of LDA-mediated imine lithiations uncovered three general mechanisms loosely depicted by transition structures **23**–**25**.^{6d,e,22} Although LDA is a disolvated dimer (**26**) in a wide range of solvents at all experimentally accessible concentrations,²³ rate studies showed that simple *N*-isopropyl ketimines lithiate via transiently formed monosolvated monomers as depicted generically by **23**. Semiempirical computational studies provided some evidence that a syn lithiation might be competitive.^{6f} LDA/THF-mediated lithiations of an imine bearing a potentially chelating *N,N*-dimethylamino appendage revealed little influence of the Me₂N moiety on the relative rates or rate law for the lithiation,^{6d,e} suggesting that the dimethylamino moiety is unable to compete with THF for coordination to lithium (**24**). (This is not completely correct, as shown below.) By contrast, lithiations of potentially chelating imines using LDA solvated by poorly coordinating trialkylamines proceed via a dimer-based transition structure suggested to be a solvent-free open dimer **25**.^{6d,e} We will demonstrate below that chelation by the potentially chelating *N*-alkyl moiety depends on other substituents within the substrate.

Results

Reagents and Starting Materials. The LDA generated from diisopropylamine and *n*-BuLi was recrystallized.²⁴ Condensations of amines and ketones to form imines followed standard literature procedures.²⁵ The 2,6,6-trideuterated and 2,2,6,6-tetradeuterated analogues were prepared from 2,6,6-trideuterio-

- (11) Fustero, S.; de la Torre, M. G.; Jofre, V.; Carlon, R. Q.; Navarro, A.; Fuentes, A. S.; Cario, J. S. *J. Org. Chem.* **1998**, *63*, 8825. Larcheveque, M.; Cuvigny, T.; Normant, H. *Synthesis* **1975**, 256. Ahlbrecht, H.; Von Daacke, A. *Synthesis* **1984**, 610. Bunnelle, W. H.; Singam, P. R.; Narayanan, B. A.; Bradshaw, C. W.; Liou, J. S. *Synthesis* **1997**, 439. Katritzky, A. R. M.; Fang, Y.; Donkor, A.; Xu, J. *Synthesis* **2000**, 2029.
- (12) A report of an anti lithiation may derive from selective destruction of the lithioimine derived from the predominant syn lithiation: Salgado, A.; Boeykens, M.; Gauthier, C.; Declercq, J.-P.; De Kimpe, N. *Tetrahedron* **2002**, *58*, 2763.
- (13) Meyers, A. I.; Williams, D. R.; Erickson, G. W.; White, S.; Druelinger, M. *J. Am. Chem. Soc.* **1981**, *103*, 3081.
- (14) Heathcock, C. H. In *Comprehensive Carbanion Chemistry*; Buncl, E., Durst, T., Eds.; Elsevier: New York, 1980; Vol. B, Chapter 4. Evans, D. A. In *Asymmetric Synthesis*; Morrison, J. D., Ed.; Academic Press: New York, 1983; Vol. 3, Chapter 1. Evans, D. A. *Aldrichimica Acta* **1982**, *15*, 23. d'Angelo, J. *Tetrahedron* **1976**, *32*, 2979.
- (15) Hosomi, A.; Araki, Y.; Sakurai, H. *J. Am. Chem. Soc.* **1982**, *104*, 2081. Welch, J. T.; Seper, K. W. *J. Org. Chem.* **1986**, *51*, 120. Welch, J. T.; Seper, K. W. *J. Org. Chem.* **1988**, *53*, 2991. Hayes, J. F.; Shipman, M.; Twin, H. *J. Org. Chem.* **2002**, *67*, 935. Evans, D. A. *J. Am. Chem. Soc.* **1970**, *92*, 7593. Hart, T. W.; Guillochon, D.; Perrier, G. Sharp, B. W.; Toft, M. P.; Vacher, B.; Walsh, R. J. A. *Tetrahedron Lett.* **1992**, *33*, 7211.
- (16) For computational studies as well as a detailed discussion of syn alkylations of imines and syn–anti isomerizations of lithioimines, see: Glaser, R.; Streitwieser, A. *J. Org. Chem.* **1991**, *56*, 6612. Glaser, R.; Streitwieser, A. *J. Org. Chem.* **1991**, *56*, 6625. For other computational studies, see: Pratt, L. E.; Hogen-Esch, T. H.; Khan, I. M. *Tetrahedron* **1995**, *21*, 5955. Stork, G.; Polt, R. L.; Li, Y.; Houk, K. N. *J. Am. Chem. Soc.* **1988**, *110*, 8360.
- (17) Houk, K. N.; Strozzi, R. W.; Rondan, N. G.; Fraser, R. R.; Chuaqui-Offermans, N. *J. Am. Chem. Soc.* **1980**, *102*, 1426.
- (18) Fraser, R. R.; Chuaqui-Offermans, N.; Houk, K. N.; Rondan, N. G. *J. Organomet. Chem.* **1981**, *206*, 131.

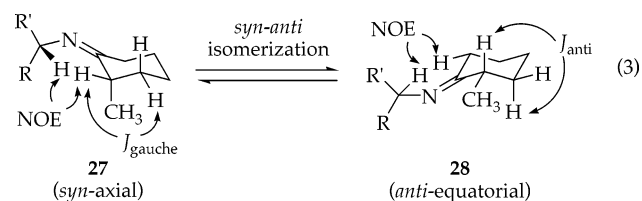
- (19) Fraser, R. R.; Banville, J.; Dhawan, K. L. *J. Am. Chem. Soc.* **1978**, *100*, 7999.
- (20) For computational studies of axial versus equatorial deprotonation of cyclohexanones, see: Behnam, S. M.; Behnam, S. E.; Ando, K.; Green, N. S.; Houk, K. N. *J. Org. Chem.* **2000**, *65*, 8970. Bordwell, F. G.; Scamehorn, R. G. *J. Am. Chem. Soc.* **1968**, *90*, 6749. Abou Rachid, H.; Larriou, C.; Chaillet, M.; Elguero, J. *Tetrahedron* **1983**, *39*, 1307.
- (21) Huff, B. J. L.; Tuller, F. N.; Caine, D. *J. Org. Chem.* **1969**, *34*, 3070. House, H. O.; Umen, M. *J. Org. Chem.* **1973**, *38*, 1000. Kahne, D.; Gut, S.; DePue, R.; Mohamadi, F.; Wanat, R. A.; Collum, D. B.; Clardy, J.; Van Duyne, G. *J. Am. Chem. Soc.* **1984**, *106*, 4685.
- (22) Rutherford, J. L.; Hoffmann, D.; Collum, D. B. **2002**, *124*, 264. Qu, B.; Collum, D. B., unpublished.
- (23) Galiano-Roth, A. S.; Collum, D. B. *J. Am. Chem. Soc.* **1989**, *111*, 6772. Galichrist, J. H.; Collum, D. B. *J. Am. Chem. Soc.* **1992**, *114*, 794. Collum, D. B. *Acc. Chem. Res.* **1993**, *26*, 227.
- (24) Kim, Y.-J.; Bernstein, M. P.; Galiano-Roth, A. S.; Romesberg, F. E.; Fuller, D. J.; Harrison, A. T.; Collum, D. B.; Williard, P. G. *J. Org. Chem.* **1991**, *56*, 4435.



2-methylcyclohexanone and 2,2,6,6-tetradeuteriocyclohexanone²⁶ (respectively) using deuterated ammonium salts (RND_3Cl) to ensure >97% isotopic enrichment.^{6d,e}

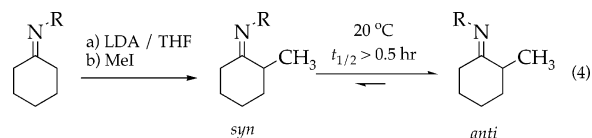
Structures of Imines. We must first describe how the imines in Chart 1 were prepared and characterized using representative examples and relying heavily on the Supporting Information. Syn and anti orientations of the *N*-alkyl moieties in imines have been assigned on the basis of ^{13}C chemical shifts and simple NOE studies.^{3,27} We used a more contemporary approach that included combinations of ^1H , ^1H -NOESY, ^1H , ^1H -COSY, and ^1H , ^1H -*J*-resolved spectroscopies.²⁸ The conformational assignments are consistent with long-standing conformational principles and are supported by density function theory (DFT) computations (see the Supporting Information).²⁹

Several conformational issues are germane to the forthcoming mechanistic discussion. First, the imines substituted by a secondary *N*-alkyl group are suggested to reside in the rotamers that place the methine hydrogen atom proximate to the equatorial hydrogen on the cyclohexane—depicted generically in **27** and **28**—so as to minimize $A_{1,3}$ strain.²⁹ Second, the imines derived from 2-methylcyclohexanone are either syn-axial (**27**) or anti-equatorial (**28**). The syn versus anti orientations are readily ascertained by the NOEs indicated. The distinction of axial and equatorial protons follows directly from the magnitudes of the coupling constants.



The assignments of the syn–anti stereochemistry require elaboration. Five pairs of isomers—**7/8**, **9/10**, **11/12**, **13/14**, and **15/16**—are interconverted by syn–anti isomerization (eq 3). Syn imine **9**, prepared >95% stereochemically pure by lithiation (LDA/THF) and syn-selective alkylation (MeI),^{10,16} was shown to be of general structure **27** using the 2-D NMR spectroscopies described above. On standing in THF at 35 °C, **9** isomerizes to predominantly anti imine **10** (general structure **28**) with $t_{1/2} \approx$

1 h. The neat oil and solutions in THF contain **9** and **10** as a 1:10 mixture. Curiously, samples in CDCl_3 equilibrate substantially faster and contain only a 1:3 mixture of **9** and **10** as noted.³⁰ Syn and anti isomers **11** and **12** were prepared and characterized using analogous methods.³¹ Imines **7** and **8** were prepared from 4-*tert*-butylcyclohexanone as a 1:1 mixture. Unfortunately, the anticipated NOE between the syn-axial proton at the 2-position of the cyclohexane and the methyl moiety on the *N*-alkyl side chain of imine **8** was too small to detect. It is presumed, using analogy to computations described herein and computations of the analogous ketone enolizations,²⁰ that the more reactive isomer is the one requiring axial deprotonation. (The preference for axial deprotonation will be discussed below.)



Imines **13–16**, corresponding to syn–anti pairs of two diastereomers, were initially prepared as a four-component mixture by treating racemic 2-methylcyclohexanone with (*S*)-2-amino-1-methoxypropane. A 1:10:1:10 mixture was observed by ^{13}C NMR spectroscopy in either THF solution or as the neat oil consistent with equilibrium populations containing low concentrations of syn isomers (**13** and **15**) and high concentrations of anti isomers (**14** and **16**).³² CDCl_3 solutions contain a 1:3:1:3 mixture, consistent with the reduced anti selectivity noted in the simpler cases above. The **13/15** and **14/16** pairs were distinguished as follows. Sequential lithiation and alkylation of imine **4** affords what was shown by the bevy of NMR spectroscopies to be a 6:1 mixture of syn-axial imines **13** and **15**. Hydrolysis without allowing intervening syn–anti isomerization afforded predominantly (*S*)-2-methylcyclohexanone (4:1 er),¹³ confirming the relative stereochemistry of the stereogenic center on the cyclohexanone moiety and the *N*-alkyl side chain of **13** and **15**. On standing at 35 °C, the 6:1 mixture of **13** and **15** isomerized ($t_{1/2} = 6$ h) predominantly to the anti isomer (**14/16** = 4:1). Hydrolysis of the isomerized material afforded (*S*)-2-methylcyclohexanone with limited epimerization (3.4:1 er). Overall, **13** and **15** can be prepared stereoisomerically enriched. As shown below, the lithiation of **16** can be easily monitored in a **13–16** mixture. The most elusive imine, **15**, can only be formed as a minor component of a four-component mixture.

Rates of Syn–Anti Isomerization. To summarize the details above, isomerization of the syn and anti isomers routinely occurs with half-lives of 6–10 h at room temperature consistent with literature reports.^{3,8,31} The isomerization is most readily observed by monitoring the equilibration of the syn isomers available by alkylation.^{3,10} Under all circumstances studied, the lithiations proved to be fast as compared to the isomerizations, allowing lithiation rates to be ascertained for syn and anti isomers independently.³³

(30) Knorr, R. *Chem. Ber.* **1980**, *113*, 2441.

(31) The equilibration of **11** and **12** is measurably faster than that of **9** and **10**, for example, as evidenced by a $t_{1/2}$ of approximately 0.5 h at 20 °C and 1.0 h at 35 °C, respectively.

(32) A similar mixture was observed for an imine derived from 2-methylcyclohexanone: Kosmrlj, J.; Weigel, L. O.; Evans, D. A.; Downey, C. W.; Wu, J. *J. Am. Chem. Soc.* **2003**, *125*, 3208.

(33) Although, in principle, some ill-defined species in the reaction could facilitate syn–anti exchange, this would manifest equivalent rates and regioselectivities for the lithiations of the syn and anti isomers.

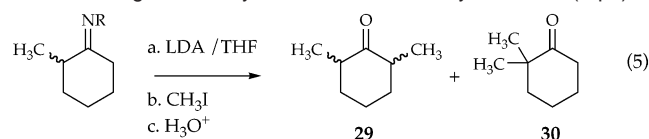
(25) Larock, R. C. *Comprehensive Organic Transformations*; VCH: New York, 1989; p 758.

(26) Peet, N. P. *J. Labelled Compd.* **1973**, *9*, 721.

(27) Fraser, R. R.; Akiyama, F.; Banville, J. *Tetrahedron Lett.* **1979**, 3929. Oliveros, E.; Riviere, M.; Lattes, A. *Org. Magn. Reson.* **1976**, *8*, 601. Also, see refs 10a,c and 19.

(28) *NMR Spectroscopy Techniques*; Bruch, M. D., Ed.; Dekker: New York, 1996.

(29) Johnson, F. *Chem. Rev.* **1968**, *68*, 375.

Table 1. Regioselectivity of Imine Lithiations by LDA/THF (eq 5)^a

entry	starting material		product 29:30 ^c	temp, time (°C, h)	reference
	compd	syn/anti ^b			
1	9	>20:1	>100:1	0, 1.5	
2	9:10	1:10	1:4.2	15, 13	
3	10	1:>20	1:8.0 ^d		calcd (entries 1,2)
4	11	>20:1	>100:1	-65, 1.0	
5	11:12	1:10	1:1.4	-40, 0.8	
6	12	1:>20	1:1.8 ^d		calcd (entries 4,5)
7	13:15^e	>20:1	>100:1	-40, 1.0	
8	13:14:15	1:10:1	1:2.4	-20, 0.8	
9	14	1:>20	1:5.5 ^d		calcd (entries 7,8)
10	13:14:15:16	1:10:1:10	1:2.0	15, 7.0	
11	16	1:>20	1:1.6 ^d		calcd (entries 7–10)

^a Reactions were carried out under pseudo-first-order conditions as described in the text. ^b Numerical ratios are obtained from ¹³C NMR spectra. ^c Ratios obtained from gas chromatography. ^d Calculated from the regioselectivity of the corresponding syn isomer and the mixture of syn/anti isomers. ^e **13:15** = 6:1.

Regioselectivity of Lithiation. The regioselectivities of the lithiations were measured by quenching the lithioimines with MeI, hydrolyzing the imine with pH 4.5 buffer,¹³ and measuring the ratio of 2,6-dimethylcyclohexanone (**29**) and 2,2-dimethylcyclohexanone (**30**) by GC (eq 5, Table 1).³⁴ The alkylations were fast at -78 °C as shown by in situ IR spectroscopy.³⁵ Moreover, the regioselectivities arose from kinetically controlled lithiation. For example, solutions of 6-lithio-2-methylcyclohexanone imines derived from the syn-oriented imines **9** or **13** do not equilibrate to provide the 2-lithio derivatives on standing in the absence or presence of unlithiated imine at 25 °C. Limited (1%) proton transfer was observed by letting the anion derived from **6** and unlithiated **12** stand at 20 °C for 2.0 h. The regioselectivities for lithiations of imines with a simple *N*-alkyl group syn to the 2-methyl moiety are measured directly using substrates available from the highly syn-selective alkylation. In contrast, the regioselectivities for the anti imines (entries 3 and 6) are extracted from results derived from 1:10 syn–anti mixtures (entries 2 and 5) by factoring out the contributions from the minor syn isomers (entries 1 and 4). Regioselectivities for **13**–**16** included an additional layer of complexity. The regioselectivity for the lithiation of **13** is measured using a highly enriched sample of **13** (with 15% **15**) available by syn alkylation (Table 1, entry 7). The regioselectivity for the three imines that lithiate quickly (**13**–**15**; entry 8), in conjunction with an exhaustive lithiation (**13**–**16**; entry 10), provides the regioselectivity for **16** (entry 11). The regioselectivity derived from **14** and **15** cannot be extracted. However, if one assumes by analogy to the other syn imines **9** and **11** (supported by the computations) that **15** lithiates with total anti selectivity, then the selectivity for **14** (entry 9) can be extracted.

(34) Alkylations of **11** and **12** both show 40–60% 2-methylcyclohexanone after hydrolysis that could derive from *N*-alkylation. This could cause some distortion in the reported regioselectivities.

(35) (a) Sun, X.; Collum, D. B. *J. Am. Chem. Soc.* **2000**, *122*, 2452. (b) Rein, A. J.; Donahue, S. M.; Pavlosky, M. A. *Curr. Opin. Drug Discovery Dev.* **2000**, *3*, 734.

Table 2. Rate Data for Imine Lithiations

compound	temp (°C)	THF order ^a	LDA order	isotope effect
1	-40			
2	0	0	0.54 ± 0.02	10 ± 1
3	-78	0 ^b	0.58 ± 0.04	9 ± 1
4	-65	0	0.59 ± 0.03	14 ± 4
5	-40	0		12 ± 2
6	-78	0		8 ± 1
7	-78	0 ^b		8 ± 1
8	-78	0 ^b		23 ± 4
9	0	0	0.49 ± 0.04	9 ± 1
10^c	20	0	0.49 ± 0.02	8 ± 2
11	-65	0 ^b	0.57 ± 0.05	1.5 ± 0.2
12	-40	0	0.51 ± 0.02	2.6 ± 0.1
13	-40	0 ^b	0.55 ± 0.05	11 ± 2
14	-20	0	0.50 ± 0.05	12 ± 2
15	-20			
16	15	0 ^b	0.56 ± 0.01	5.3 ± 0.4
31^c	0	0	0.55 ± 0.03	>5
32	-40	0	0.51 ± 0.03	

^a The zeroth orders were determined by visual inspection rather than by numerical fit (Figure 3). ^b Reaction rates increase at low THF concentration. ^c From a previous study.^{6e}

Inspection of the syn–anti ratios and the regioselectivities (Table 1) indicates that the regioselectivities are determined largely, but not entirely, by the orientation of the *N*-alkyl groups. Syn imines **9**, **11**, and **13** show a strong preference for lithiation anti to the *N*-alkyl moiety because anti lithiation also corresponds to lithiation at the less substituted (methylene) carbon. Anti imines **10**, **12**, **14**, or **16** lithiate predominantly anti to the *N*-alkyl moiety despite the requisite unfavorable lithiations at the more substituted 2-position to provide 2,2-dimethylcyclohexanone. (The impact of lithiation geminal to the methyl is discussed below.) However, the 10–40% lithiation at the less substituted sites cannot be derived solely from the 10% contamination by the syn isomers. It would appear, therefore, that some syn lithiation must be occurring. Logically, the regioselectivities derived from syn–anti mixtures depend on the extent of lithiation attributable to the rapid lithiation of the minor syn isomers followed by the substantially slower lithiation of the major anti imines.

Kinetics: General Methods. Rate studies of the LDA/THF-mediated lithiations provide a foundation to understand the substituent effects. Pseudo-first-order conditions were achieved by setting the initial concentrations of imines at 0.005 M. The LDA and THF were maintained at high, yet adjustable, concentrations using hexane as the cosolvent.³⁶ The lithiations were monitored using in situ IR spectroscopy by following the loss of the imine absorbance at 1652–1667 cm⁻¹ as described.^{6e} The resulting pseudo-first-order rate constants (*k*_{obsd}) are independent of the initial concentration of imine, confirming the first-order dependence.³⁷ Isotope effects measured using 2,2,6-trideuterated and 2,2,6,6-tetradeuterated substrates (Table 2), despite the considerable range (*k*_H/*k*_D = 1.5–23), point to a rate-limiting proton transfer.^{6d,e,38}

Kinetics: Relative Rate Constants. The relative rate constants (*k*_{rel}) listed in Chart 1 were determined from the values of *k*_{obsd} measured under pseudo-first-order conditions as described above. Lithiation rates for imines **1**, **2**, **5**, and **12**–**14**

(36) The concentration of the lithium amide, although expressed in units of molarity, refers to the concentration of the monomer unit (normality).

(37) Espenson, J. H. *Chemical Kinetics and Reaction Mechanisms*; McGraw-Hill: New York, 1995; p 15.

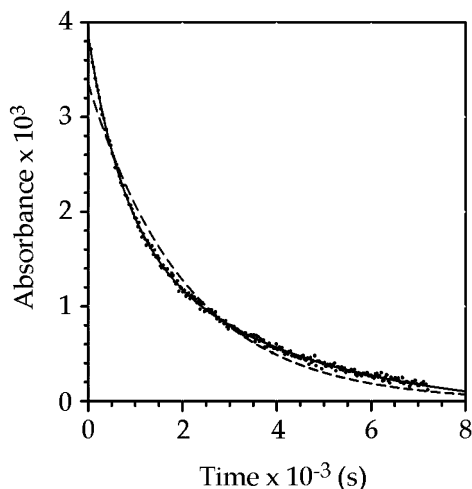


Figure 1. Biphasic decay of the lithiation of a 1:1 mixture of imines **7** and **8** (total concentration: 0.005 M) by LDA (0.13 M) in THF (12.2 M) at $-78\text{ }^{\circ}\text{C}$. The decay was fit to (1) $y = a[\exp(-k_{\text{obsd}}t)]$ (--- line), $k_{\text{obsd}} = (6.0 \pm 0.1) \times 10^{-4}$; (2) $y = a[\exp(-k_7t) + \exp(-k_8t)]$ (solid line), $k_7 = (1.53 \pm 0.08) \times 10^{-3}$, $k_8 = (3.4 \pm 0.2) \times 10^{-4}$.

were measured directly at $-40\text{ }^{\circ}\text{C}$. Especially reactive substrates (**3**, **4**, **6–8**, and **11**) and relatively unreactive substrates (**9**, **10**, and **16**) were monitored at two temperatures and extrapolated to $-40\text{ }^{\circ}\text{C}$. Rate studies described below reveal that all lithiation rates are independent of the THF concentrations at $>5.0\text{ M}$ THF (see the Supporting Information). Imines **1–6** presented no technical challenges beyond the temperature extrapolations. Measuring the relative rate constants of the other imines demanded varying degrees of innovation as follows.

In principle, a 1:1 mixture of **7** and **8** might display biphasic kinetics (see below) due to differential lithiation rates. Indeed, the loss of the IR absorbance at 1663 cm^{-1} corresponding to the **7/8** mixture displayed a deviation from a clean first-order decay in which the initially high rates in the first half-life give way to attenuated rates in the remaining half-lives as shown by the dotted line in Figure 1. Alternatively, the data were fit to the expression

$$[\text{imine}]_{\text{total}} = [\mathbf{7}]_0 \exp(-k_7t) + [\mathbf{8}]_0 \exp(-k_8t)$$

(k_7 and k_8 correspond to the rate constants for lithiation of **7** and **8**), affording an excellent fit. (The curve is obscured by the data points in Figure 1.) Because **7** and **8** could not be distinguished spectroscopically, we rely on computational evidence described herein and elsewhere²⁰ to attribute the approximate 5-fold difference to the preferred axial lithiation of **7** as compared to the equatorial lithiation of **8** (vide infra).

Lithiation of anti imine **10**, contaminated by 10% syn isomer **9**, was monitored directly by IR spectroscopy. The relatively rapid lithiation of **9** at the outset allowed **10** to be monitored independently. By contrast, the syn imine **9** was prepared isomerically pure by the syn-selective alkylation protocol but could not be isolated without intervening isomerization to **10**.

(38) The small isotope effects for **11** and **12** could be interpreted as evidence of a rate-limiting syn–anti isomerism as suggested previously.¹⁰ The LDA-concentration-dependent rate constants argue against such a mechanism due to the dependence of regioselectivity on syn/anti orientation in the substrate. Moreover, we have noted surprisingly low isotope effects in the LDA-mediated lithiation of the dimethylhydrazone of cyclohexanone, in which symmetry renders syn–anti isomerism irrelevant. Collum, D. B.; Romesberg, F. E., unpublished.

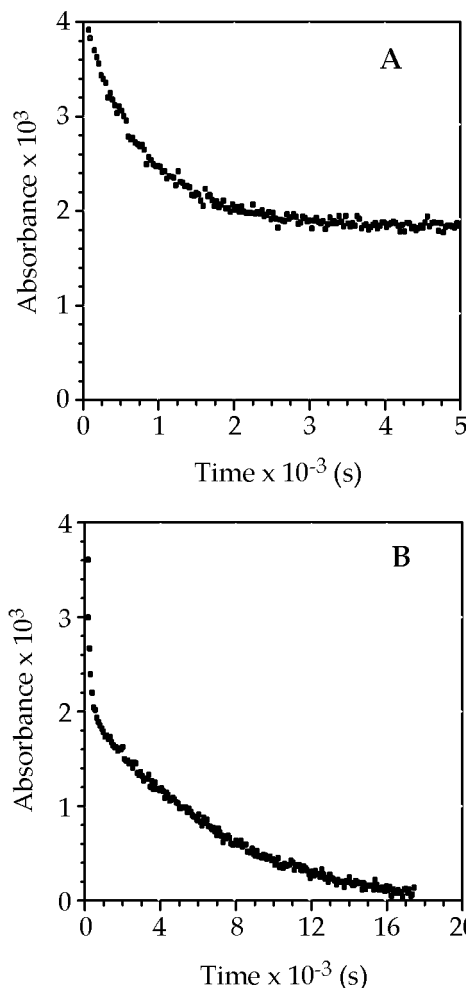


Figure 2. Biphasic decay of the lithiation of a 1:10:1:10 mixture of imines **13**, **14**, **15**, and **16** (total concentration: 0.005 M) by LDA (0.13 M) in THF (12.2 M). (A) $-20\text{ }^{\circ}\text{C}$; the decay was fit to $y = \exp(-k_{\text{obsd}}t) + c$, $k_{\text{obsd}} = (1.3 \pm 0.5) \times 10^{-3}$, used as k_{obsd} of **14**; (B) $15\text{ }^{\circ}\text{C}$; the decay (excluding points from the first 600 s) was fit to $y = \exp(-k_{\text{obsd}}t) + c$, $k_{\text{obsd}} = (1.3 \pm 0.2) \times 10^{-4}$.

Consequently, concentrated solutions of **9** generated in situ were injected without workup or warming into solutions of LDA. The small amounts of LiI or other contaminants could, in principle, influence the rate of lithiation. Nonetheless, an analogous sample of imine **10** generated by alkylation followed by warming to $25\text{ }^{\circ}\text{C}$ (to effect syn-to-anti isomerization) displays the same reactivity as samples of **10** injected as a neat oil. The relative rate constants for **11** and **12** were determined using analogous methods.

Measuring the relative rate constants for the lithiation of **13–16** proved challenging. The lithiations of a 1:1 mixture of **14** and **16** (contaminated by low concentrations of syn imines **13** and **15** discussed above) showed striking biphasic kinetics. The lithiation followed a first-order decay to 50–60% conversion at $-20\text{ }^{\circ}\text{C}$ due to rapid lithiation of **14** (Figure 2A) as well as the low concentrations of **13** and **15**. Alternatively, lithiation at $15\text{ }^{\circ}\text{C}$ proceeded immediately to 50–60% conversion due to the nearly instantaneous lithiation of **13–15** followed by a first-order loss of the remaining imine corresponding to the lithiation of **16** (Figure 2B). Therefore, the lithiation rates of **14** and **16** were measured independently. Monitoring the lithiations by ^{13}C NMR spectroscopy confirmed that the $^{13}\text{C}=\text{N}$ resonances of

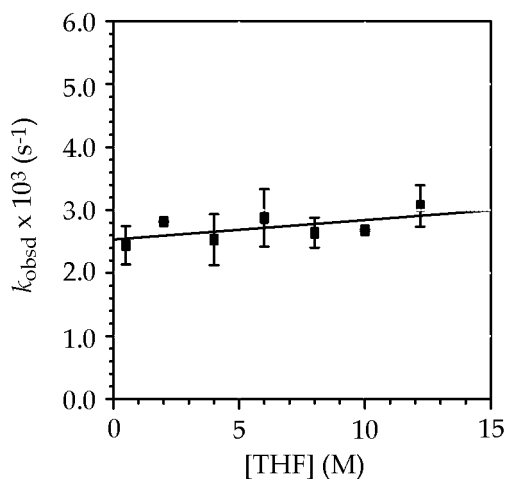


Figure 3. Plot of k_{obsd} versus free [THF] in hexane for the lithiation of **4** (0.005 M) by LDA (0.13 M) at -65 °C. The line depicts an unweighted least-squares fit to $k_{\text{obsd}} = k[\text{THF}] + k'$ ($k = (3 \pm 2) \times 10^{-5}$, $k' = (2.5 \pm 0.1) \times 10^{-3}$).

13–15 begin to disappear at -20 °C, whereas the $^{13}\text{C}=\text{N}$ resonance of **16** decreases measurably at 15 °C.

The syn imine **13**, prepared through a syn alkylation (with a 15% contamination by **15**), was further lithiated without warming or isolation (as noted for **9** above). The loss of **13** proceeds to full conversion by a standard first-order decay. Once again, a control experiment indicates that samples of imine generated in situ are well behaved. Thus, if **13** is prepared in situ, isomerized to anti isomer **14** by warming (with approximately 10% epimerization of **13** to **16**), and then lithiated by excess LDA, we obtain the same rate constant ($\pm 10\%$) as that obtained for the lithiation of **14** added to LDA as a neat oil.

The most difficult relative rate constant to measure was that of syn imine **15**, available only as a minor component in a mixture of **13–16**. By following the loss of the four isomers by ^{13}C NMR spectroscopy, we could show that syn imine **15** lithiates at approximately the same rate as anti isomer **14**. The NMR spectroscopic experiment also qualitatively confirmed the relative lithiation rates of all four imines.

Kinetics: Rate Laws. We have argued vehemently that relative rate constants are of limited value in the absence of detailed rate studies showing mechanistic homo- or heterogeneity.^{6e} The protocol used to determine a number of rate laws is described below using the lithiation of **4** emblematically. The results are summarized in Table 2.

A plot of k_{obsd} versus THF concentration with hexane as cosolvent (Figure 3) reveals a zeroth-order dependence on THF concentration consistent with a lithiation that involves neither dissociation nor association of THF from dimer **26** leading to the rate-limiting transition structure.³⁹ A plot of k_{obsd} versus LDA concentration shows a clean half-order dependence (Figure 4, Table 2) consistent with a dimer–monomer preequilibrium.³⁹ The rate data are described by the idealized rate law in eq 6 and are consistent with monomer-based transition structure $[(i\text{-Pr}_2\text{NLi})(\text{THF})(\mathbf{4})]^\ddagger$.

$$-\text{d}[\text{imine}]/\text{d}t = k[\text{imine}][\text{LDA}]^{1/2}[\text{THF}]^0 \quad (6)$$

In several of the more reactive methoxy-substituted cases—**3**, **7/8**, **11**, **13**, and **16**—plots of k_{obsd} versus THF concentration

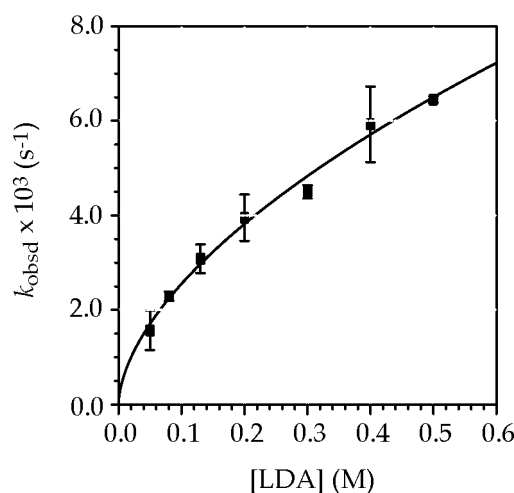


Figure 4. Plot of k_{obsd} versus [LDA] in THF (12.2 M) for the lithiation of **4** (0.005 M) at -65 °C. The curve depicts an unweighted least-squares fit to $k_{\text{obsd}} = k[\text{LDA}]^n$ ($k = (9.8 \pm 0.4) \times 10^{-3}$, $n = 0.59 \pm 0.03$).

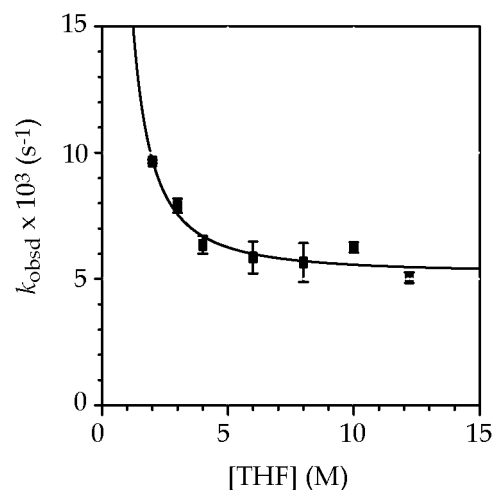


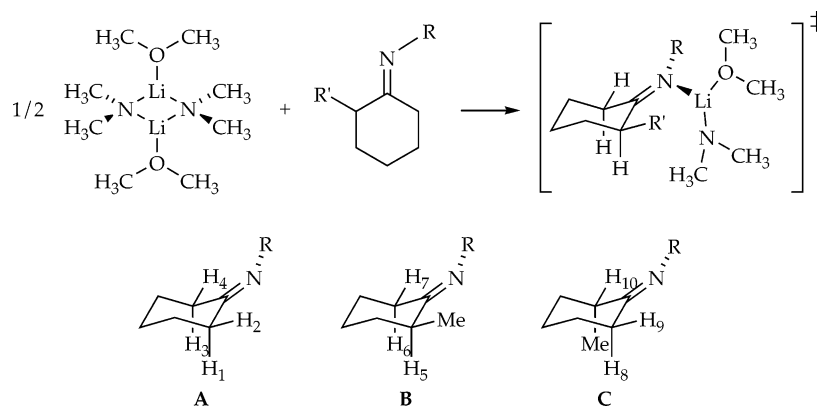
Figure 5. Plot of k_{obsd} versus free [THF] in hexane for the metalation of **3** (0.005 M) by LDA (0.13 M) at -78 °C. The curve depicts an unweighted least-squares fit to $k_{\text{obsd}} = k[\text{THF}]^n + k'$ ($k = (1.4 \pm 0.5) \times 10^{-2}$, $k' = (5.2 \pm 0.6) \times 10^{-3}$, $n = -1.6 \pm 0.6$). The reaction is zeroth order in THF at high [THF].

show increases in the rates at low THF concentrations (Figure 5). These rate spikes are attributable to pathways requiring dissociation of one or more coordinated THF. Because such THF concentration-dependencies are confined to only the lowest THF concentrations, we were unable to probe the details of that pathway. We suspect, however, that the rate spikes at very low THF concentrations derive from previously observed open dimer-based lithiations (analogous to **25**). We hasten to add that the dissociative pathways do not measurably influence the relative rate constants in Chart 1, nor do they influence the mechanistic discussions below. Projected investigations using less strongly coordinating solvents should be revealing.

The biphasic kinetics noted in a previous section for the lithiation of the **14/16** mixture afforded the two term rate law described by eq 7. (k_{14} and k_{16} correspond to the rate constants for lithiation of **14** and **16**.) The term for lithiation of imine **14** was determined at -20 °C, whereas that for the lithiation of imine **16** was determined at 15 °C. The concentration-dependencies (Table 2) are consistent with monosolvated monomer-

(39) Edwards, J. O.; Greene, E. F.; Ross, J. J. *Chem. Educ.* **1968**, *45*, 381.

Scheme 2



based transition structures, $[(i\text{-Pr}_2\text{NLi})(\text{THF})(\text{imine})]^\ddagger$ in both cases. The relative rate constants, however, provide compelling evidence of substantial mechanistic differences (see below).

$$-d[\text{imine}]/dt = (k_{14}[\mathbf{14}] + k_{16}[\mathbf{16}])[\text{LDA}]^{1/2}[\text{THF}]^0 \quad (7)$$

Kinetics: Me₂N-Substituted Imines Revisited. Previous rate studies of the LDA/THF-mediated lithiations of imine **31/32** (1:1) containing a pendant Me₂N moiety afforded rates and a rate law that were indistinguishable from those of *N*-isopropyl analogue **10**.^{6d,e} The apparent first-order decay led us to conclude that diastereomers **31** and **32** lithiate with equal facility. Moreover, we concluded that the lithiation proceeds via transition structure **24** with the pendant Me₂N moiety unable to compete with THF for coordination to lithium. On the basis of the results for the analogous mixture of methoxy-substituted imines **14** and **16** showing striking biphasic kinetics, we suspected that we may have missed the lithiation of **32**. This oversight is readily understood by noting that previous rate studies were carried out using transmission IR spectroscopy rather than in situ IR spectroscopy. The contents of the reaction vessel were fixed at either 0 or 25 °C and pumped through the IR cell using approximately 1.0 m of intramedic tubing, rendering the first 20–30 s of the reaction spectroscopically invisible.

We reinvestigated the lithiation of the **31/32** mixture and indeed found that the diastereomers lithiated at >200-fold different rates by LDA/THF. The slow-reacting imine **31** behaves indistinguishably from *N*-isopropyl analogue **10**, consistent with transition structure **33**. In contrast, the fast-reacting form lithiates readily at ≤ −40 °C. Detailed rate studies of this fast-reacting form (Table 2) are consistent with a monomer-based transition structure $[(i\text{-Pr}_2\text{NLi})(\text{THF})(\text{imine})]^\ddagger$, which we depict as transition structure **34** bearing a chelating Me₂N moiety. Thus, the rate law previously reported for the lithiation of the **31/32** mixture is actually the rate law for the lithiation of the slow-reacting imine **31**.

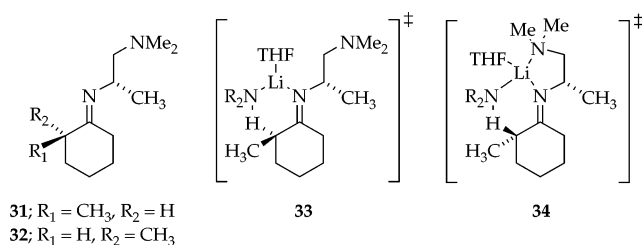


Table 3. Activation Energies (ΔG^\ddagger , kcal/mol) for the Lithiation of Imines **A**, **B**, and **C** (Scheme 2) Calculated with B3LYP/6-31G(d)

Compd.	ΔG^\ddagger	R =					
		CH ₃	<i>i</i> -Pr	<i>i</i> -Pr	2-H	2-(<i>S</i>)-CH ₃	2-(<i>R</i>)-CH ₃ ^a
A	ΔG^\ddagger_1	20.8	23.1	17.0	18.0	--	--
	ΔG^\ddagger_2	21.8	--	19.1	20.4	--	--
	ΔG^\ddagger_3	26.2	--	20.0	19.8	--	--
	ΔG^\ddagger_4	28.1	--	22.2	22.2	--	--
B	ΔG^\ddagger_5	22.6	26.2	19.9	--	21.1	26.1 (27.8) ^b
	ΔG^\ddagger_6	26.6	--	20.8	--	21.2	31.7 (31.3) ^b
	ΔG^\ddagger_7	29.0	--	24.7	--	--	24.8
C	ΔG^\ddagger_8	21.9	23.2	19.3	--	19.8	25.6 (24.2) ^b
	ΔG^\ddagger_9	24.0	--	19.4	--	28.1	21.3
	ΔG^\ddagger_{10}	34.7	--	28.4	--	--	--

^a Structures of **B** and **C** with 2-(*R*)-methyl are not shown in Scheme 2.

^b Methoxy group is not coordinated to the lithium in the transition structure.

DFT Computational Studies. We explored the origin of the structure-dependent regioselectivities and relative rates using DFT calculations performed with the 6-31G* basis set at the B3LYP level of theory.⁴⁰ Me₂NLi and Me₂O were used as models for LDA and THF, respectively.⁴¹ A range of initial geometries were sampled for all reactant and transition structures. Legitimate saddle points were shown by the existence of a single imaginary frequency. Corrections for the Gibbs free energy (ΔG) are included. The structures and energies for cyclohexanone- and 2-methylcyclohexanone-derived imines of general form **A**, **B**, and **C** (Scheme 2) are included in the Supporting Information. Optimized transition structures of stoichiometry $[(\text{Me}_2\text{NLi})(\text{Me}_2\text{O})(\text{imine})]^\ddagger$ for the abstraction of the 10 different protons (labeled H₁–H₁₀ on **A**–**C**) are also archived in the Supporting Information. The calculated activation energies (ΔG^\ddagger 's) are summarized in Table 3. A select group of transition structures are depicted in Figures 6 and 7.

The selected geometric details of the calculated structures **i**–**viii** are listed in Table 5. All calculated C–H–N bond angles

- (40) Frisch, M. J.; Trucks, G. W.; Schlegel, H. B.; Scuseria, G. E.; Robb, M. A.; Cheeseman, J. R.; Zakrzewski, V. G.; Montgomery, J. A., Jr.; Stratmann, R. E.; Burant, J. C.; Dapprich, S.; Millam, J. M.; Daniels, A. D.; Kudin, K. N.; Strain, M. C.; Farkas, O.; Tomasi, J.; Barone, V.; Cossi, M.; Cammi, R.; Mennucci, B.; Pomelli, C.; Adamo, C.; Clifford, S.; Ochterski, J.; Petersson, G. A.; Ayala, P. Y.; Cui, Q.; Morokuma, K.; Malick, D. K.; Rabuck, A. D.; Raghavachari, K.; Foresman, J. B.; Cioslowski, J.; Ortiz, J. V.; Baboul, A. G.; Stefanov, B. B.; Liu, G.; Liashenko, A.; Piskorz, P.; Komaromi, I.; Gomperts, R.; Martin, R. L.; Fox, D. J.; Keith, T.; Al-Laham, M. A.; Peng, C. Y.; Gill, A.; Nanayakkara, C.; Gonzalez, M.; Challacombe, P. M. W.; Johnson, B.; Chen, W.; Wong, M. W.; Andres, J. L.; Gonzalez, C.; Head-Gordon, M.; Replogle, E. S.; Pople, J. A. *Gaussian 98*; Gaussian, Inc.: Pittsburgh, PA, 1998.
- (41) Romesberg, F. E.; Collum, D. B. *J. Am. Chem. Soc.* **1992**, *114*, 2112. Ramirez, A.; Collum, D. B., unpublished.

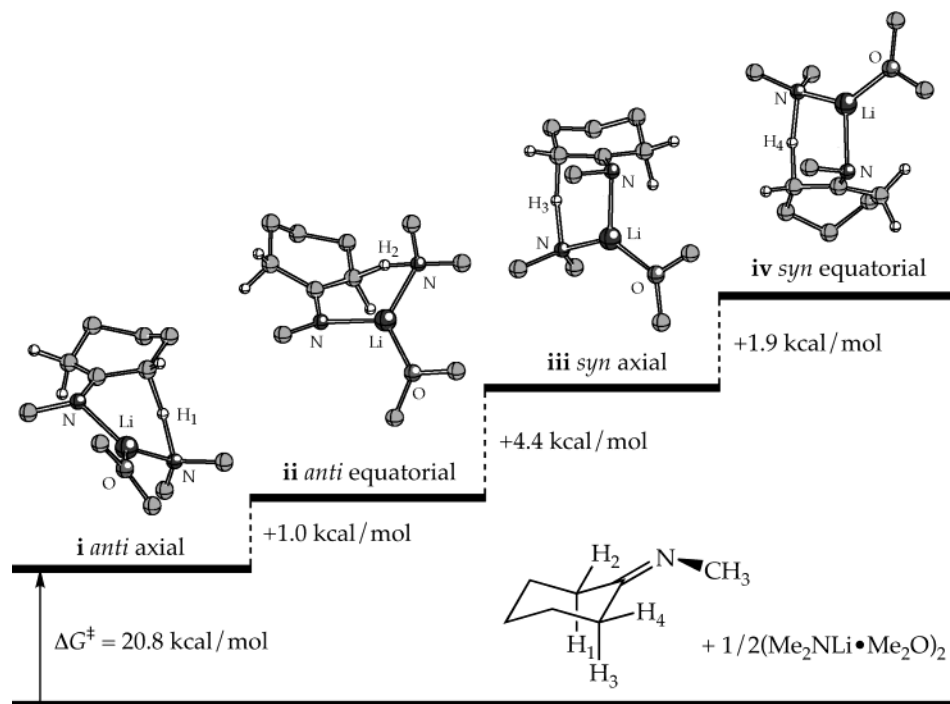


Figure 6. Transition structures and activation energy diagram of Me₂NLi-mediated metalation of *N*-methyl imine of cyclohexanone.

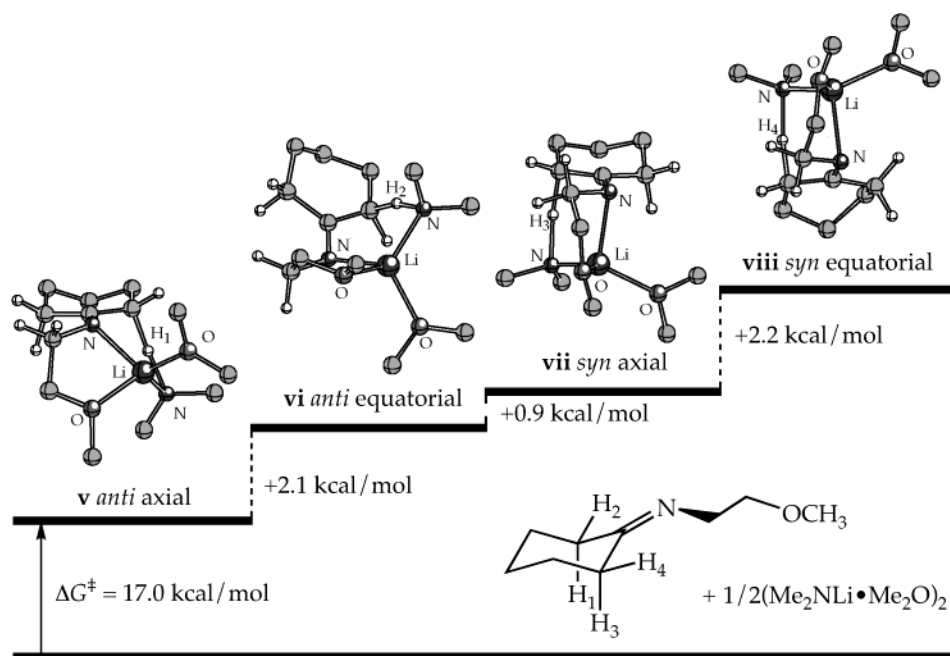


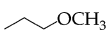
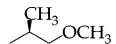
Figure 7. Transition structures and activation energies of the Me₂NLi-mediated metalation lithiation of the *N*-methoxyethyl imine of cyclohexanone.

fall in a narrow 160–170° range with relatively invariant C–H and N–H distances. As one might expect, the C–H and C=N bonds are longer than those found in the imines consistent with fractional bonding. The lithium in the syn lithiations orients more nearly perpendicular to the C=N-containing plane than does the lithium in the anti lithiations as evidenced by the C–C–N–Li dihedral angles more closely approximating 90°. The syn structures also show H–C–C–N dihedral angles approaching 90°, allowing the C–H bond to be collinear with the p-orbitals of the C=N π system. The anti structures show a shorter N–H bond, possibly emblematic of a more advanced proton transfer. Therefore, the syn lithiations show geometries that seem

intuitively more in line with stereoelectronic principles, yet this is not manifested in the calculated energies.

The calculated activation energies provide insight into the relative facilities of proton abstraction (1) syn versus anti to the *N*-alkyl group, (2) axial versus equatorial on the cyclohexane, (3) geminal to a methyl moiety versus a proton, and (4) distal to an axial methyl versus a proton. Of the 55 possible comparisons of ΔG^\ddagger 's in Table 3, a select group of especially pertinent examples are listed in Table 4. The general structure–reactivity relationships will be exploited to provide insights into the structure-dependent rates, regioselectivities, and kinetic resolutions.⁴²

Table 4. Selected Comparisons of Calculated Activation Energies (kcal/mol) for the Lithiations of Imines **A**, **B**, and **C** (Scheme 2) from Table 3

Topic	Entry	ΔG^\ddagger	R = CH ₃				
			2-H	2-(S)-CH ₃	2-(R)-CH ₃ ^a		
axial vs equat.	1	$\Delta G_{2-}^\ddagger - \Delta G_{1-}^\ddagger$	1.0	2.1	2.4	--	--
	2	$\Delta G_{4-}^\ddagger - \Delta G_{3-}^\ddagger$	1.9	2.2	2.4	--	--
	3	$\Delta G_{7-}^\ddagger - \Delta G_{6-}^\ddagger$	2.4	3.9	--	--	-6.9
	4	$\Delta G_{9-}^\ddagger - \Delta G_{8-}^\ddagger$	2.1	0.1	--	8.3	-4.3
syn vs anti	5	$\Delta G_{3-}^\ddagger - \Delta G_{1-}^\ddagger$	5.4	3.0	1.8	--	--
	6	$\Delta G_{4-}^\ddagger - \Delta G_{2-}^\ddagger$	6.3	3.1	1.8	--	--
	7	$\Delta G_{7-}^\ddagger - \Delta G_{5-}^\ddagger$	4.0	0.9	--	0.1	5.6
	8	$\Delta G_{10-}^\ddagger - \Delta G_{9-}^\ddagger$	10.7	9.0	--	--	--
2-H vs 2-CH ₃	9	$\Delta G_{5-}^\ddagger - \Delta G_{1-}^\ddagger$	1.8	2.9	--	2.1	8.1
	10	$\Delta G_{8-}^\ddagger - \Delta G_{1-}^\ddagger$	1.1	2.3	--	1.8	7.6
2-CH ₃	11	$\Delta G_{9-}^\ddagger - \Delta G_{2-}^\ddagger$	2.2	0.3	--	7.7	0.9
	12	$\Delta G_{6-}^\ddagger - \Delta G_{3-}^\ddagger$	0.4	0.8	--	1.4	11.9
	13	$\Delta G_{7-}^\ddagger - \Delta G_{4-}^\ddagger$	0.9	2.5	--	--	2.6
	14	$\Delta G_{10-}^\ddagger - \Delta G_{4-}^\ddagger$	6.6	6.2	--	--	--

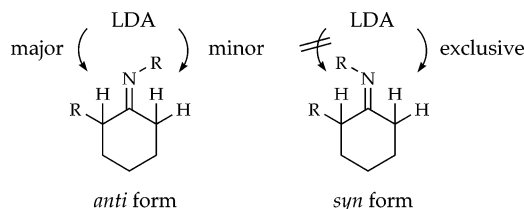
^a Nonchelating transition structures are not included.

Discussion

The organolithium chemistry of ketimines and aldimines has been investigated largely from a substrate-centric perspective in which the nuances of the underlying organometallic chemistry are largely ignored.^{1–3,18} Conversely, our previous studies follow an organolithium-centric approach in which the imines are simply exploited as templates to study issues of solvation and aggregation.⁶ It appears naive in retrospect to have believed that an approach philosophically biased in either direction could adequately explore frequently observed odd stereo- and regioselectivities and substrate-dependent rates exemplified in Scheme 1 and Chart 1. By studying a range of relatively simple substrates (**1–12**), we sought to understand how structural features within the imines influence their reactivities. Do these structure–reactivity relationships then allow us to understand the odd selectivities in Scheme 1 and relative reactivities of imines **13–16**? Before this point is addressed, some of the more germane observations are summarized as follows.

Regioselectivities. The LDA-mediated lithiation highlighted in Scheme 1 exhibited a 3:1 preference for lithiation at the more substituted α -carbon as well as a 75:1 relative reactivity of the two diastereomers. A more comprehensive investigation of regioselectivity (Table 1) provides some useful details. Imines prepared directly from 2-methylcyclohexanone exist as approximate 1:10 syn/anti mixtures both in THF solution and as neat oils (eq 4; Table 1, entries 2 and 5). The syn and anti isomers both lithiate several orders of magnitude faster than a potentially competing syn–anti equilibration, allowing the regioselectivities and lithiation rates to be determined independently. As summarized pictorially below, the observed regioselectivities were attributed to (1) a totally regioselective lithiation anti to the *N*-alkyl moiety of the syn form, and (2) an attenuated (≤ 9 :1) regioselective lithiation anti to the *N*-alkyl moiety in the anti form. Although the regioselectivities in Table 1 were determined by indirect methods in some cases, it is clear that the lithiations display a high, but not total, anti selectivity. The seemingly sporadic reversals in regioselectivity reported^{10,13,15} are easily understood as deriving from varying proportions of the syn and anti forms which, in turn, depend

on whether the substitutionally unsymmetrical imines were prepared from unsymmetrical ketones or by alkylation of imines derived from symmetric ketones. These results are consonant with those from the groups of Bergbreiter, Newcomb, and Meyers.¹⁰



Mechanism of Lithiation. The results from detailed rate studies are summarized in Table 2. In short, the rate laws are all of a mathematical form (eq 6) consistent with lithiation via monosolvated monomers. At risk of stating the obvious, the rate studies do not offer insights into geometric details such as whether (1) a pendant methoxy moiety chelates at the transition structure, (2) deprotonation occurs from an axial or equatorial site, or (3) lithiation occurs syn or anti relative to the *N*-alkyl moiety. The rate laws do, however, serve the critical function of confining computational studies and mechanistic discussions to transition structures bearing a single, well-defined stoichiometry—[(*i*-Pr)₂NLi](THF)(imine)[‡].³⁹ Of course, it is much simpler to explore relative reactivities of the four α protons on a computer than in the lab. The synergies arising from the structural, rate, and computational studies are central to unraveling the complex structure–reactivity relationships.

Caveats. Before specific structure–reactivity relationships are discussed, it seems prudent to digress briefly by mentioning a few misconceptions that often emerge at the murky interface where prose and thermochemistry meet.

First, it is easy to be fooled by seemingly large relative rate constants. For example, although the difference in relative rate constants for **7** ($k_{\text{rel}} = 44\,000$) and **8** ($k_{\text{rel}} = 8100$) may seem vastly different on first inspection, their relative magnitudes are a modest 5.4:1, corresponding to only 0.8 kcal/mol at $-40\text{ }^\circ\text{C}$. The reactivities of **5** ($k_{\text{rel}} = 190$) and **2** ($k_{\text{rel}} = 120$) are essentially indistinguishable.

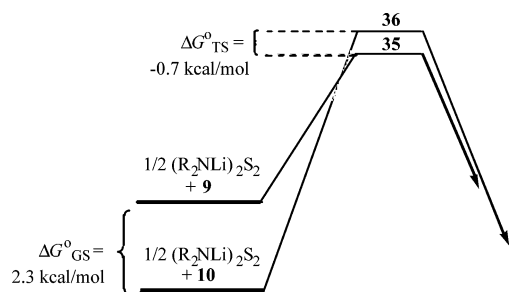
Second, there is an insidious phenomenon that we facetiously refer to as the “universal ground-state assumption”^{6c} that seems to arise from confusion over the distinction of “relative transition state energies” versus “relative activation energies”. In short, it is surprisingly common for authors to ignore the role of ground-state energies when discussing reactivity. By doing so, one implicitly (and quite erroneously) assumes that reactants are of a common energy. The 7-fold greater rate for the lithiation of syn imine **9** as compared to anti isomer **10** is illustrative. Because syn and anti imines generally do not equilibrate at the temperatures of the lithiations (rendering the Curtin Hammett principle not at issue), it might be tempting to focus on divergent steric or electronic effects in putative transition structures **35** and **36** to explain the higher reactivities of syn imine **9** as compared to those of anti isomer **10**. However, if one considers the relative energies of the reactants (as determined by their populations at equilibrium), one finds that isomeric transition structures **35** and **36** are of nearly equal energy. Consequently, the relative lithiation rates of **9** and **10** derive almost entirely from the relative stabilities of imines **9** and **10** rather than the

(42) For excellent references and discussions of kinetic resolutions, see: *Acc. Chem. Res.* **2000**, issue No. 6.

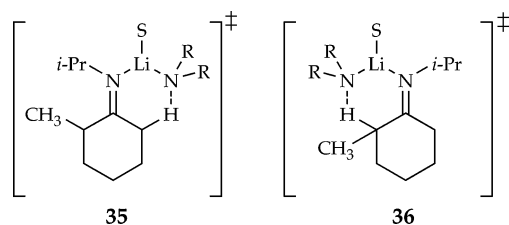
Table 5. Selected Bond Lengths, Bond Angles, and Dihedral Angles for Calculated Transition Structures i–viii (Figures 6 and 7)

parameter ^a	i	ii	iii	iv	v	vi	vii	viii
Bond Lengths (Å)								
C1–C2	1.45	1.45	1.53	1.53	1.45	1.45	1.53	1.53
C1–C3	1.53	1.52	1.45	1.45	1.53	1.53	1.45	1.45
C1–N1	1.33	1.32	1.32	1.32	1.32	1.32	1.32	1.32
C2–H	1.35	1.35			1.33	1.32		
C3–H			1.34	1.31			1.33	1.31
N2–H	1.42	1.42	1.47	1.51	1.45	1.45	1.47	1.51
N1–Li	2.00	1.99	2.09	2.08	2.07	2.06	2.23	2.21
N2–Li	1.96	1.96	1.96	1.95	1.98	2.00	1.98	1.98
O1–Li (v–viii)					2.08	2.09	2.02	2.03
O2–Li	1.93	1.93	1.91	1.91	1.99	2.02	1.98	1.98
Bond Angles (deg)								
C2–H–N1	162.6	165.5			163.8	165.3		
C3–H–N1			165.3	166.3			167.0	168.1
N1–Li–N2	115.2	116.0	112.4	112.3	110.0	107.3	107.1	106.4
N2–Li–O2	127.4	124.2	134.9	135.2	117.7	120.4	120.8	121.4
O2–Li–N1	117.1	119.6	112.7	112.5	111.6	119.5	109.3	110.0
O1–Li–N1 (v–viii)					83.8	82.6	83.7	83.9
O1–Li–N2 (v–viii)					119.4	123.3	122.2	122.2
O1–Li–O2 (v–viii)					109.4	98.5	107.0	106.0
Dihedral Angles (deg)								
H–C2···C1···N1	62.9	58.9			64.9	61.5		
H–C3···C1···N1			74.5	72.2			72.9	69.9
C2···C1···N1–Li	30.9	30.5			40.9	39.8		
C3···C1···N1–Li			79.7	78.2			77.2	76.8

^a C2 = *anti*-C α , C3 = *syn*-C α , N1 = nitrogen of imine, N2 = nitrogen of lithium amide, O1 = oxygen of chelating methoxy group, O2 = oxygen of dimethyl ether.

**Figure 8.** Thermochemistry for lithiation of **9** and **10**.

energies of their respective transition structures **35** and **36** (Figure 8). Of course, although one can compare relative activation energies for the reaction of fundamentally different substrates, it is invalid to discuss the relative energies of two transition states that are not isomeric or related by a balanced equation.



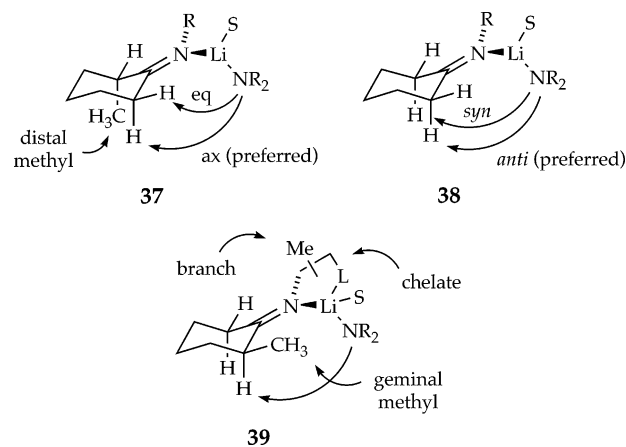
Contributions to Rates: Theory versus Experiment. With the aid of both experimentally observed rate constants and computationally determined activation energies, we can at least partially dissect the observed rates and selectivities into six components as summarized in Table 6 and illustrated generically by **37**–**39**. Thermochemical dissections are often difficult both scientifically and linguistically because the components are superimposed and can be correlated. Nevertheless, by focusing on the lithiations of simple imines **1**–**12**, we discover some

Table 6. Contributions to Imine Reactivity: Theory versus Experiment^a

entry	contribution	theory		experiment (–40 °C)	
		kcal/mol	source ^b	kcal/mol	source ^c
1	axial vs equatorial	1.0–2.4	4 (1, 2)	0.8	7/8
2	<i>syn</i> vs <i>anti</i>	1.8–6.3	4 (5, 6)	2.2–3.2 ^d	10 and 12 ^d
3	chelation	2.6–6.3	3 (1–10) ^e	1.8–2.4	1/3, 2/4
4	geminal methyl	1.8–2.9	4 (9)	1.9–2.2	2/10, 3/12
5	branched <i>N</i> -alkyl	0.0–2.4	3 (1–4) ^f	0.4–1.1	1/2, 3/4
6	distal (axial) methyl	1.1–2.3	4 (10)	0.9–1.3	2/9, 3/11
7	distal (equat) methyl	0.4–0.8	4 (12)		

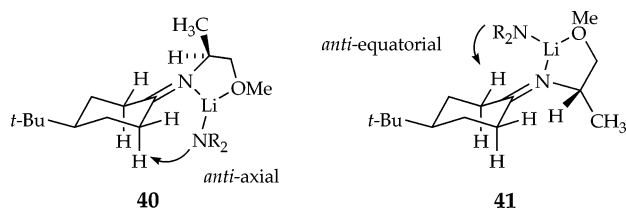
^a Comparisons exclude complex imines **13**–**16**. ^b Table number (entry numbers). ^c Compound numbers in Chart 1 used to calculate experimental contributions ($\Delta G = -RT \ln(k_1/k_2)$, $T = -40$ °C). ^d Calculated from regioselectivities of **10** and **12** (Table 1, entries 3 and 6) and geminal methyl effect (Table 6, entry 4, 1.9–2.2 kcal/mol). This value does not include provisions for the distal equatorial methyl. ^e Comparing Me versus CH₂CH₂OCH₃ and *i*-Pr versus CH(CH₃)CH₂OCH₃ in Table 3. ^f Comparing Me versus *i*-Pr and CH₂CH₂OCH₃ versus CH(CH₃)CH₂OCH₃ in Table 3.

interesting patterns that help us understand the more complex lithiations of imines **13**–**16**.



(1) Axial versus equatorial: Representative anti-axial, anti-equatorial, syn-axial, and syn-equatorial deprotonations are illustrated by the calculated transition structures and free energy diagrams in Figures 6 and 7. A significant (1.0–2.4 kcal/mol) preference for axial over equatorial deprotonation (cf., entries 1 and 2 in Table 4; see 37) is predicted regardless of whether the deprotonation occurs syn or anti to the *N*-alkyl group and regardless of whether the *N*-alkyl forms a chelate.

Isotopic labeling studies could, at least in principle, delineate the preference for axial versus equatorial deprotonation; however, the challenges confronted in preparing the labeled isomers due to imine–enamine tautomerization were too daunting. Nonetheless, conformationally anchored substrates **7** and **8** provide tacit evidence that axial deprotonation is preferred. Given the strong evidence that chelation is involved (discussed below), the high conformational control imparted by A-strain forces the preferred anti lithiations of **7** and **8** to occur from the axial and equatorial sites, respectively, as illustrated in **40** and **41**. Given the 1:1 ratio of **7** and **8**,⁴³ the approximate 5-fold higher rate for the lithiation of **7** reflects a 5-fold preference for axial proton abstraction (~0.8 kcal/mol at –40 °C). Thus, the theory and experiment are in qualitative agreement, although the calculations using Me₂NLi/Me₂O as a model appear to overestimate the stereoelectronic effect.



(2) Syn versus anti: Transition structures **i–viii** (Figures 6 and 7) and the affiliated ΔG^\ddagger 's (Table 3, ΔG_1^\ddagger – ΔG_4^\ddagger) provide perspectives of syn versus anti deprotonations (see 38). Comparing syn versus anti deprotonation via the preferred axial mode (Table 4, entry 5) is most germane and shows a distinct anti selectivity. Although the selectivity is attenuated by both branching on the *N*-alkyl group and methyl substitution on the cyclohexane ring (Table 4, entry 7; vide infra), lithiation anti to the *N*-alkyl group is predicted for all cases.

The experimental results are consistent with the computations. The regioselectivities listed in Table 1 show a substantial preference for deprotonation anti to the *N*-alkyl moiety. Syn imines **9** and **11** undergo a totally regioselective anti deprotonation at the less-substituted site (Table 1, entries 1 and 3). Anti isomers **10** and **12** undergo predominantly anti lithiation despite the requisite deprotonation at the more substituted position. Imines **10** and **12** undergo a small but measurable syn lithiation as well.

(3) Chelated versus nonchelated: The presence of a potentially chelating methoxy moiety on the *N*-alkyl group (see 39) appears to be the largest determinant of reactivity.⁴⁴ Comparing calculated ΔG^\ddagger 's for simple imines (Table 3, R = Me)⁴⁵ and the chelating imines (Table 3, R = CH₂CH₂OMe) reveals a

predicted 2.6–6.3 kcal/mol reduction in activation energy for the chelated forms. The most pertinent comparison—the chelated versus nonchelated anti-axial deprotonation via transition structures **i** and **v** (Figures 6 and 7)—shows a 3.8 kcal/mol lower ΔG_1^\ddagger for the chelated form (Table 3, entry 1). Moreover, chelation is predicted to accelerate the syn lithiations (**vii**) more so than the anti lithiations (cf., R = Me versus CH₂CH₂OMe; Table 4, entry 5), suggesting that chelation might cause a reduction in regioselectivity.

Although rate studies do not distinguish chelated versus nonchelated forms in the transition structures, the accelerations imparted by the potentially chelating side chains, in conjunction with the computational studies, leave little doubt that chelation occurs at the transition structure. By example, the 200-fold higher reactivity of imine **4** when compared to **2** (corresponding to 2.4 kcal/mol at –40 °C) certainly attests to the importance of the methoxy moiety. Similarly, the methoxy group on imine **3** causes an approximate 40-fold acceleration by comparison to the *n*-butyl group of **1**. Moreover, the regioselectivities in Table 1 suggest that the methoxy moiety of imine **12** erodes the anti selectivity (entry 6) when compared to the *N*-isopropyl group of imine **10** (entry 3), although the loss of regioselectivity is less than predicted computationally.

(4) Geminal methylation: Introducing a methyl moiety at the 2-position of the cyclohexane provides a regiochemical tag but also retards the lithiation (see 39). Calculations suggest that a geminally disposed methyl group in the equatorial position causes the ΔG^\ddagger 's for the preferred anti-axial lithiation to increase by 1.8–2.9 kcal/mol (Table 4, entry 9). Indeed, the lithiation of **10**, which occurs predominantly geminal to the methyl, is 120 times slower (2.2 kcal/mol at –40 °C) than the lithiation of its unsubstituted counterpart **2**, which matches the calculated value of 3.1 kcal/mol (cf., ΔG_1^\ddagger and ΔG_5^\ddagger for *i*-Pr in Table 3). Similarly, the lithiation of **3** is predicted computationally to be 2.9 kcal/mol more favorable than the lithiation of **12** (Table 4, entry 9), whereas experimentally an approximate 60-fold greater rate (1.9 kcal/mol at –40 °C) is observed.

(5) Distal methylation: To understand the regioselectivity, one must also understand how lithiation at the 6-methylene group is influenced by a distal 2-methyl substituent (see 37). If the *N*-alkyl group is anti to the 2-methyl moiety (as in general structure **B**; Scheme 2), syn lithiation at the CH₂ position is calculated to be slower than the syn lithiation in the unsubstituted case (Table 4, entry 12). However, the 2-methyl group in **B** is predicted to retard the anti lithiation (Table 4, entry 9) more so than the syn lithiation.

Lithiations of the syn-axial imines of general structure **C** prefer anti-axial lithiation at the unsubstituted CH₂ position despite the distal methyl moiety (Table 4, entry 4). The ΔG^\ddagger 's for the anti-axial deprotonations are predicted to be inhibited by only 1.1–2.3 kcal/mol due to the axial distal methyl (Table 4, entry 10).⁴⁶ Thus, imines with the *N*-alkyl group syn to the 2-methyl moiety are predicted to lithiate rapidly and with a high selectivity to the less-substituted side.

Comparing the relative rates in Chart 1 for **2** versus **9** ($k_{\text{rel}} = 17$; 1.3 kcal/mol at –40 °C) and **3** versus **11** ($k_{\text{rel}} = 6.8$; 0.9 kcal/mol at –40 °C), we find that syn imines of general structure **C** display reactivities that are intermediate between the anti

(43) The calculated relative energies of two isomers corresponding to **7** and **8** with the *tert*-butyl group omitted show a 0.2 kcal/mol preference for **8**. (Without the *tert*-butyl group, there are still two isomers.)

(44) For examples and leading references, see: Ramírez, A.; Collum, D. B. *J. Am. Chem. Soc.* **1999**, *121*, 11114.

(45) The calculated ΔG_1^\ddagger for imine **1** bearing an *n*-butyl group is 21.9 kcal/mol.

(46) In fact, computational studies of the lithiation of **2** and **9** (Table 3) show no difference in ΔG_8^\ddagger versus ΔG_1^\ddagger due to the distal methyl.

Table 7. Contributions to Relative Rates for Lithiation of Imines **13**–**16** Scaled to Imine **3**

contribution	estimated relative free energies of activation (kcal/mol)					
	$\Delta G_{\text{rel}}^{\ddagger}(44)$	$\Delta G_{\text{rel}}^{\ddagger}(45)$	$\Delta G_{\text{rel}}^{\ddagger}(46)$	$\Delta G_{\text{rel}}^{\ddagger}(47)$	$\Delta G_{\text{rel}}^{\ddagger}(48)$	$\Delta G_{\text{rel}}^{\ddagger}(49)$
axial vs equatorial	0	0	0.8	0.8	0	0
syn vs anti	0	0	0	2.2–3.2	2.2–3.2	0
chelation	0	0	0	0	0	1.8–2.4
geminal methyl	0	1.9–2.2	0	1.9–2.2	0	1.9–2.2
<i>N</i> -alkyl branch	0.4–1.1	0.4–1.1	0.4–1.1	0.4–1.1	0.4–1.1	0.4–1.1
distal methyl	0.9–1.3	0	0 ^b	0	0.9–1.3	0
chair–chair flip					(0.9) ^d	
predicted	1.3–2.4	2.3–3.3	1.2–1.9	5.3–7.3 ^e	4.4–6.5	4.1–5.7
observed ^a	2.1	2.8	(2.8) ^c	4.7	4.7	4.7

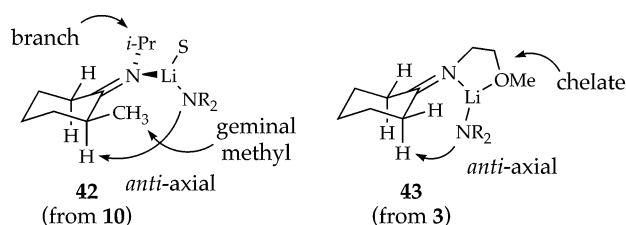
^a Scaled to -40 °C (Chart 1). ^b Distal axial methyl is on the opposite face of the cyclohexane ring. ^c Approximate. ^d Calculated energy of placing a methyl group axial from the preferred equatorial orientation in the ground state for the *N*-methylimine of cyclohexanone. ^e Cost of a syn-equatorial lithiation was estimated from the calculations to be very large (ΔG_9 , Table 3).

forms (**B**) and unsubstituted derivatives (**A**). The prohibitively high ΔG^{\ddagger} s associated with the syn-equatorial deprotonations of syn form **C** are completely borne out by the high regioselectivities for syn imines **9** and **11** (Table 1).

(6) *N*-Alkyl branching: Calculations predict that branching on the *N*-alkyl group (see **39**) retards the lithiation. For example, comparing ΔG^{\ddagger} s for the lithiation of the unsubstituted imine **A** (Table 3, entries 1–4) shows that the methyl group on the chelating side chain [R = CH(CH₃)CH₂OCH₃] is predicted to cause 0.0–2.4 kcal/mol higher activation energy. Similarly, the preferred anti-axial lithiation of *N*-isopropylcyclohexanone imine **2** is calculated to be considerably less favorable ($\Delta G_1^{\ddagger} = 23.1$ kcal/mol; Table 3) than the corresponding anti-axial lithiation of *N*-*n*-butyl-substituted imine **1** ($\Delta G^{\ddagger} = 21.9$ kcal/mol).⁴⁵

The experimentally measured relative rates show a similar effect. The lithiation of *N*-isopropylimine **2** is approximately 10 times slower than that of the *N*-*n*-butyl analogue **1**. Similarly, lithiation of **4** is 2–3 times slower than that of the unsubstituted analogue **3**.

Additives. The six identifiable contributions to the lithiation rates (listed in Table 6), although of moderate influence in isolation, display surprising additivities. The additivities are best illustrated by dissecting the experimentally derived 60 000-fold relative rates for the lithiation of imines **3** and **10** (5.1 kcal/mol at -40 °C) into the individual contributions as illustrated by **42** and **43**. Whereas both imines can undergo the preferred anti-axial lithiation, lithiation of **3** (via **43**) is facilitated by chelation (1.8–2.4 kcal/mol from Table 6) and is not inhibited by any other structural features. In contrast, the lithiation of **10** (via **42**) is inhibited by the branching in the *N*-alkyl moiety (0.4–1.1 kcal/mol) and by a geminal methyl group (1.9–2.2 kcal/mol). The predicted relative activation energies of 4.1–5.7 kcal/mol obtained by summing these contributions compare favorably to the observed value of 5.1 kcal/mol. This analysis works quite well for other binary comparisons in Chart 1. It would also work well using the computational results from Table 6 were it not for the substantial overestimate of stabilization by the chelate.

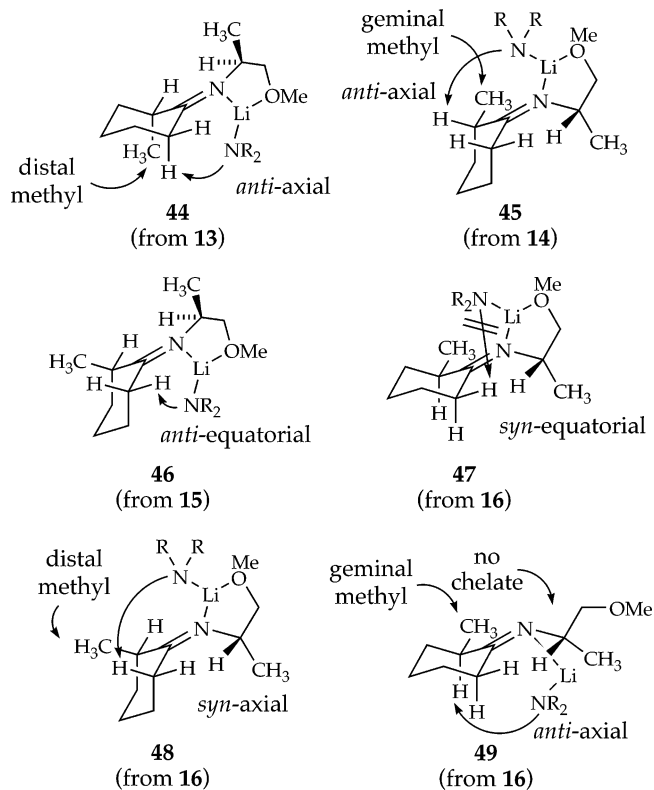


Kinetic Resolution. Having assessed the independent contributions that determine the rates of imine lithiations, we are now in a position to examine the kinetic resolution depicted in Scheme 1. The starting imine was shown to be a 1:10:1:10 mixture of imines **13**, **14**, **15**, and **16**. The relative rates in Chart 1 reveal the relative reactivities as **13** > **14** \approx **15** \gg **16**. The biphasic kinetics affiliated with a kinetic resolution in Scheme 1 arose because **13**–**15** lithiate readily at -20 °C, whereas **16** lithiates slowly at 15 °C. The individual structure–reactivity relationships gleaned from Table 6 were compiled for imines **13**–**15**, affording predicted activation energies. The results are summarized in Table 7. (The energetic contributions listed in Table 7 are scaled relative to the most reactive imine **3**.) Imines **13**–**15** are predicted to undergo facile lithiation because they suffer from only minor problems arising from a distal methyl group (see **44**), a geminal methyl group (see **45**), or a requisite equatorial deprotonation (see **46**). In contrast, a chelation-assisted lithiation of **16** is forced to proceed via a syn-equatorial deprotonation (see **47**) predicted by computations to be prohibitively poor. Alternatively, **16** could undergo a chair–chair flip (costing 0.9 kcal/mol relative to its lowest energy conformer)⁴⁷ followed by a syn-axial deprotonation (see **48**). The cost of the conformational adjustment, the syn lithiation, and the distal methyl renders the relative activation energy quite large and more than offsets any advantages offered by the chelation. Consequently, **16** appears to undergo lithiation without assistance by chelation (see **49**) to a significant extent, as evidenced by a lithiation rate that is analogous to the rate observed for the *N*-isopropyl imine **10**.

Conclusions

A recurring theme emerges in these studies: spectroscopic, computational, and rate studies function synergistically, offering views of synthetically important reactivities and selectivities that are unavailable when the methods are used in isolation. The structure-dependent rates and selectivities of LDA/THF-mediated imine lithiations highlighted in Scheme 1 and Chart 1 were traced to a combination of factors including proton abstraction (1) axial versus equatorial, (2) syn versus anti, (3) geminal to a methyl moiety, (4) distal to a methyl moiety, (5) with chelation assistance, and (6) in the presence of a branched *N*-alkyl substituent. Although many of these factors have been identified

(47) The 0.9 kcal/mol is an estimate from the value derived for the chair–chair flip of *N*,2-dimethylcyclohexanone imine. The cost of the chair–chair flip must be included because the anti-axial form is not the lowest energy conformer.



and studied previously, the selectivities and relative rates, when placed in the context of kinetic and computational studies, provides a more unified picture. From this overview emerges a model in which highly structure-dependent rates—rates that span almost 5 orders of magnitude—are shown to derive from relatively modest contributions displaying a surprising additivity.

We must confess that we began this study with the intention of investigating the previously detected dimer-based pathway fostered by weakly coordinating donor solvents. However, with the aid of new technology—in situ IR spectroscopy³⁵—it soon became apparent that some of our previous observations and conclusions, although technically not wrong, offered an incomplete picture. With a firmer understanding of the chemistry of a structurally diverse group of imines, a probe of how the

principles described herein translate to the dimer-based lithiation should be fruitful. In a more general sense, the results offer a better understanding of how the synthetically important organolithium chemistry of imines depends critically on controlling the syn–anti stereochemistry about the C=N bond. This notion is not new,⁹ but it may be underappreciated. By example, the kinetic resolution in Scheme 1, although not yet useful in its current form due to problems with regiocontrol and partial epimerization,⁴⁸ warrants further study.

Experimental Section

Reagents and Solvents. Amines and hydrocarbons were routinely distilled by vacuum transfer from blue or purple solutions containing sodium benzophenone ketyl. The hydrocarbon stills contained 1% tetraglyme to dissolve the ketyl. The LDA was prepared and purified by recrystallization as described.²⁴ Deuterated imines were prepared from the deuterated ketones²⁶ and RND₃Cl salt (to minimize loss of deuterium) as described.^{6c} Air- and moisture-sensitive materials were manipulated under argon or nitrogen using standard glovebox, vacuum line, and syringe techniques.

NMR Spectroscopic Analyses. Samples were prepared, and the ¹H and ¹³C NMR spectra were recorded as described in the Supporting Information.

IR Spectroscopic Analyses. Spectra were recorded with an in situ IR spectrometer fitted with a 30-bounce, silicon-tipped probe optimized for sensitivity as described in the Supporting Information and elsewhere.^{35a}

Acknowledgment. We thank the National Institutes of Health for direct support of this work as well as Dupont Pharmaceuticals, Merck Research Laboratories, Pfizer, Aventis, R. W. Johnson, Boehringer-Ingelheim, and Schering-Plough for indirect support. We also acknowledge the National Science Foundation Instrumentation Program (CHE 7904825 and PCM 8018643), the National Institutes of Health (RR02002), and IBM for support of the Cornell Nuclear Magnetic Resonance Facility.

Supporting Information Available: NMR spectra and rate data (PDF). This material is available free of charge via the Internet at <http://pubs.acs.org>.

JA030409Z

(48) Imine hydrolyses without epimerization have been reported: Nakamura, M.; Hatakeyama, T.; Hara, K.; Nakamura, E. *J. Am. Chem. Soc.* **2003**, *125*, 6362.